



# Electrical properties of neutron-irradiated oxygen potential sensors using stabilized zirconia solid electrolyte

N. Hiura<sup>a,\*</sup>, Y. Endo<sup>a</sup>, T. Yamaura<sup>a</sup>, T. Hoshiya<sup>a</sup>, M. Niimi<sup>a</sup>, J. Saito<sup>a</sup>,  
S. Sozawa<sup>a</sup>, N. Ooka<sup>a</sup>, M. Kobiyama<sup>b</sup>

<sup>a</sup> Department of JMTR, Oarai Research Establishment, Japan Atomic Energy Research Institute, Oarai-machi, Higashiibaraki-gun, Ibaraki-ken 311-13, Japan

<sup>b</sup> Faculty of Engineering, Ibaraki University, Hitachi, Ibaraki-ken 316, Japan

## Abstract

Oxygen sensors based on zirconia solid electrolyte stabilized by MgO, CaO or Y<sub>2</sub>O<sub>3</sub> were irradiated with neutrons in the Japan Materials Testing Reactor (JMTR) of the Japan Atomic Energy Research Institute (JAERI), and the characteristics of electromotive force of these sensors under and after irradiation were measured. The electromotive force of YSZ sample decreased with increasing irradiation fluence up to  $1 \times 10^{23} \text{ m}^{-2}$  ( $E > 1 \text{ MeV}$ ). The electromotive force of the MSZ sensor irradiated for fluences up to  $9 \times 10^{21} \text{ m}^{-2}$  ( $E > 1 \text{ MeV}$ ) was almost equal to the reference value of the electromotive force. It was shown that after irradiation, the decrease in the electromotive force of the CSZ sensor was smaller than those of MSZ and YSZ sensors, although the electromotive forces of MSZ, CSZ and YSZ sensors were smaller than the reference value. © 1998 Elsevier Science B.V. All rights reserved.

## 1. Introduction

An oxygen potential sensor is indispensable to the development of breeding materials for a fusion reactor [1,2]. It is useful to study the surface reaction of breeding materials, since the amount of H<sub>2</sub> (additions in sweep gas) absorbed in the breeding materials such as Li<sub>2</sub>O, Li<sub>4</sub>SiO<sub>4</sub>, LiAlO<sub>2</sub>, Li<sub>2</sub>ZrO<sub>3</sub> and Li<sub>2</sub>TiO<sub>3</sub> must be examined under controlled oxygen potential in the sweep gas to clarify the capability of tritium release and tritium recovery on the surface of breeding materials. The surface reaction in breeding materials is one of the key issues that control the performance of the fusion blanket with respect to tritium release and tritium recovery. The purpose of this paper is to investigate neutron irradiation effects on the electromotive force of oxygen potential sensors [3], from the view-point of capabilities of the sensor. Oxygen potential sensors based on zirconia solid

electrolyte stabilized by MgO, CaO and Y<sub>2</sub>O<sub>3</sub>, named MSZ, CSZ and YSZ [4], respectively, were irradiated with neutrons in JMTR of JAERI, and characteristic tests of oxygen sensors were carried out.

## 2. Experimental

### 2.1. Production of oxygen sensors

A schematic drawing of the oxygen sensor is shown in Fig. 1. The solid electrolytes [5–7] were made of three kinds of zirconia (supplied by the Nikkato Corporation, of dimensions 6 mm in outer diameter, 4 mm in inner diameter and 50 mm in length) which were stabilized by 11 mol% CaO, 9 mol% MgO and 8 mol% Y<sub>2</sub>O<sub>3</sub>, respectively.

The Ni/NiO reference electrode [8] was produced by mixing 99.9% Ni powder (63 μm particle size or less) and 99% purity NiO powder (about 9 μm) in the molar ratio of 7:3. For this electrode, a Ni rod of 2 mm in diameter and 50 mm in length was used.

The Fe/FeO electrode [9] was produced by mixing over 99.9% Fe powder (50 μm or less) and 99.9% FeO

\* Corresponding author. Tel.: +81 29 264 8344; fax: +81 29 264 8480; e-mail: hiura@oarai.jaeri.go.jp.

<sup>1</sup> N. Hiura is also studying in the special course of the graduate school of Ibaraki University.

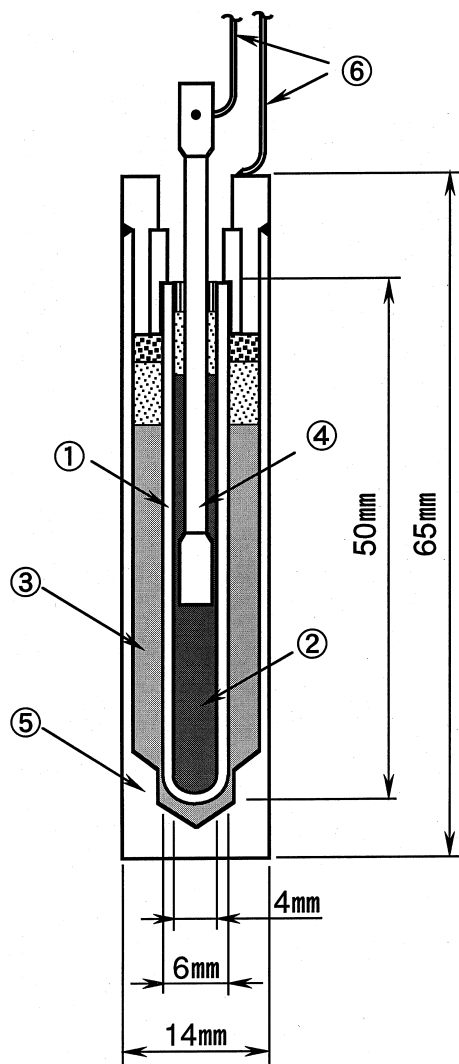


Fig. 1. Structure of oxygen sensors: (1) Solid electrolyte; (2) Ni/NiO pole; (3) Fe/FeO pole; (4) Ni electrode; (5) Cell case; (6) Ni leads.

powder (177  $\mu\text{m}$  or less) in the molar ratio of 4:1. This electrode was constructed in a cell case (14 mm of outer diameter, 60 mm of length) made of electrolytic iron.

### 2.2. In situ tests

In situ tests of the YSZ sensor were carried out in order to study the temperature dependence of electromotive force (EMF) and the changes in EMF with time under irradiation. The YSZ sensor was loaded in a capsule, and was irradiated with neutrons up to  $1.1 \times 10^{23} \text{ m}^{-2}$  ( $E > 1 \text{ MeV}$ ). The temperature of the sensor during the irradiation was about 980–1040 K, and irradiation time was 250 h. A hybrid-recorder

(Yokokawa Electronic Corporation, HR-1300) was used to measure the EMF and temperature of oxygen sensors. Time dependence of EMF is shown in Fig. 2, while temperature dependence is given in Fig. 3.

### 2.3. Post-irradiation tests

The three types of oxygen sensors were loaded into hydraulic rabbits, and were irradiated up to  $8.9 \times 10^{21}$ – $8.9 \times 10^{22} \text{ m}^{-2}$  ( $E > 1 \text{ MeV}$ ) at 503 K in JMTR. Irradiation time was 14–140 h. After irradiation, the hydraulic rabbits were disassembled in the hot laboratory of JMTR, and post-irradiation tests of oxygen sensors were carried out.

The oxygen sensors were inserted in an electric furnace in order to study the temperature dependence of the EMF, and the EMF of the oxygen sensors was repeatedly measured from 873 K to 1273 K. The test was carried out in a He gas atmosphere.

DC resistance measurements were carried out in order to study the activation energy of oxygen ion conduction. AC impedance measurements were also carried out in order to study the activation energy of the dipole of the stabilized zirconia solid electrolyte by means of an impedance-gain analyzer supplied by Sora Toron Corporation.

## 3. Results and discussions

### 3.1. In situ tests

(1) Life tests of EMF of YSZ sensors: The time dependence of EMF for the YSZ sensor under irradiation is shown in Fig. 2. The temperature of the sensor was kept constant at about 973 K during these tests. The EMF of the YSZ sensor was 231 mV at the start of the tests and decreased to 180 mV after an irradiation fluence of  $1 \times 10^{22} \text{ m}^{-2}$  ( $E > 1 \text{ MeV}$ ). After that, the EMF of the YSZ sensor increased to 216 mV at a fluence of  $5 \times 10^{22} \text{ m}^{-2}$  ( $E > 1 \text{ MeV}$ ), and then decreased to 110 mV at a fluence of  $1 \times 10^{23} \text{ m}^{-2}$  ( $E > 1 \text{ MeV}$ ).

(2) Characteristic tests of EMF of YSZ sensors: The temperature dependence of EMF of the YSZ sensor under irradiation is shown in Fig. 3. The dotted line shows the reference EMF as calculated from thermodynamic data. The EMF of unirradiated YSZ sensor was nearly equal to the theoretical EMF. When the YSZ sensor was irradiated with neutron fluences of  $1 \times 10^{22}$  and  $5 \times 10^{22} \text{ m}^{-2}$  ( $E > 1 \text{ MeV}$ ), EMF were about 0–40 mV smaller than that of the unirradiated sensor. Furthermore, when the YSZ sensor was irradiated to a neutron fluence of  $1 \times 10^{23} \text{ m}^{-2}$  ( $E > 1 \text{ MeV}$ ), the EMF was reduced to a value about 100 mV smaller than that of unirradiated sensor.

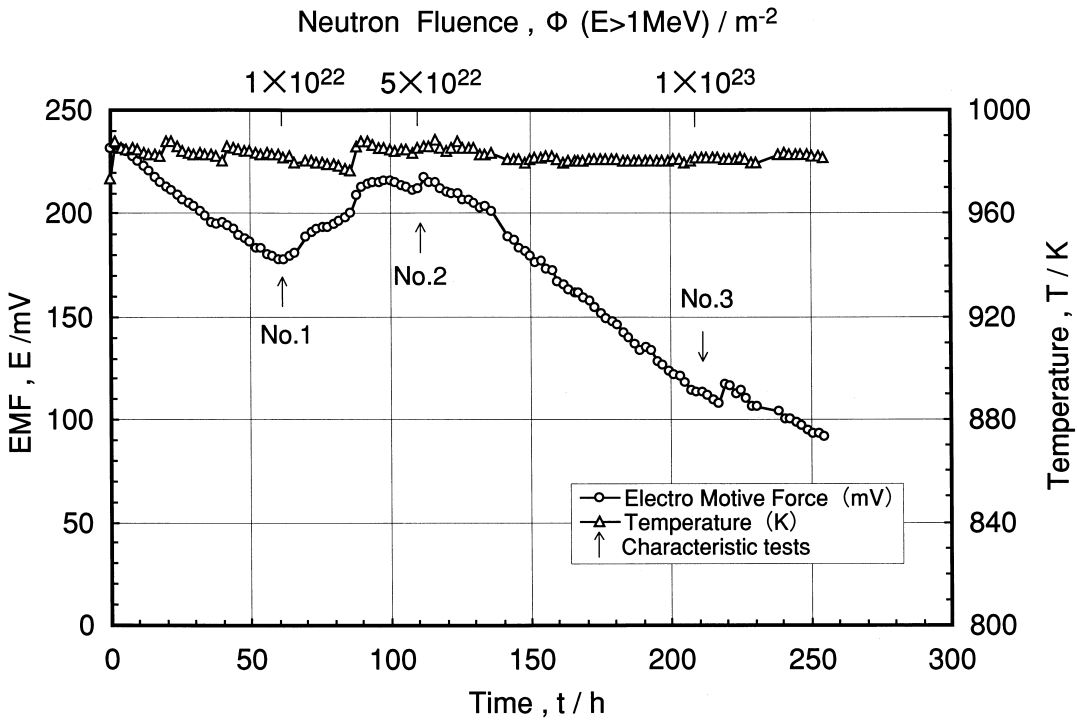


Fig. 2. Relationship between testing time and EMF under irradiation.

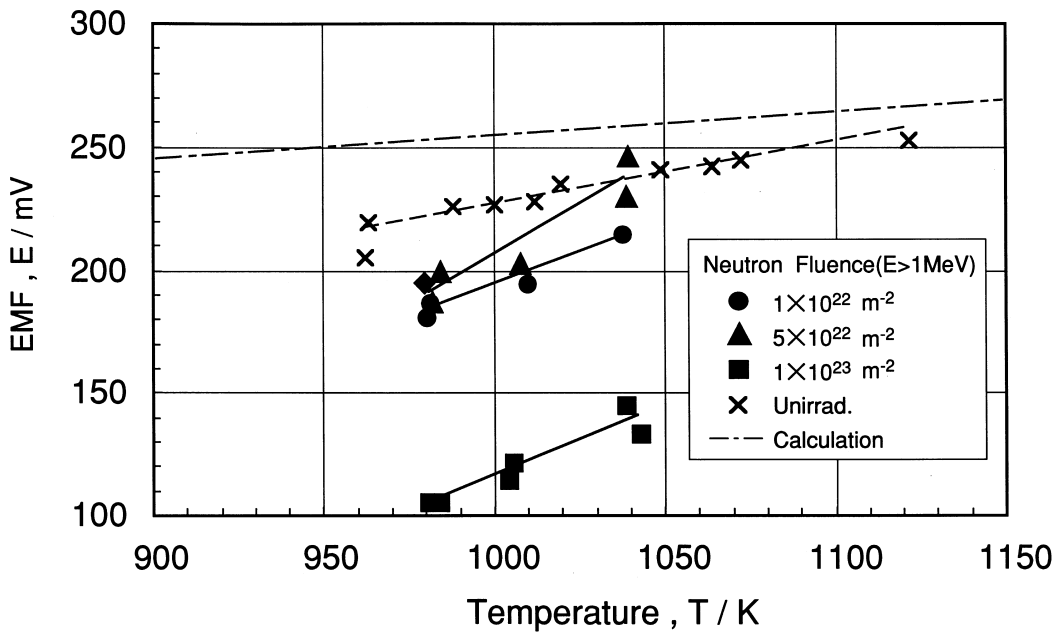


Fig. 3. Relationship between temperature and EMF under irradiation.

3.2. Post-irradiation tests

(1) Characteristic tests of EMF of oxygen sensors:  
 The temperature dependence of EMF of oxygen sensors

is shown in Fig. 4. The EMF of the MSZ sensor irradiated with neutron fluences of  $8.9 \times 10^{21} \text{ m}^{-2}$  ( $E > 1 \text{ MeV}$ ) and that of the unirradiated YSZ sensor were equal to the reference EMF calculated from

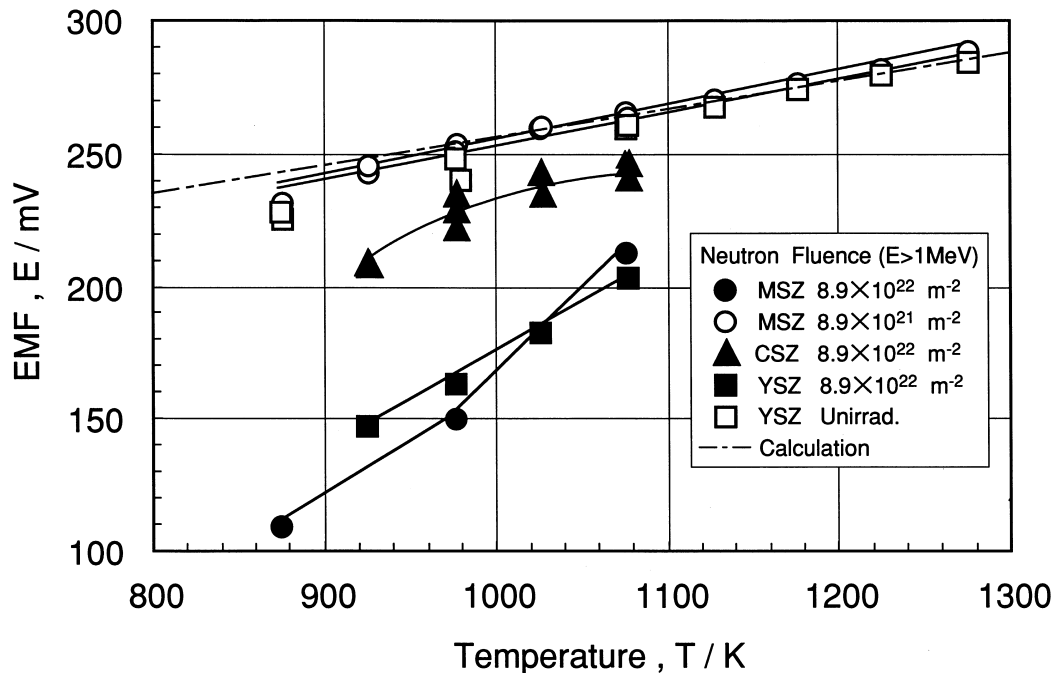


Fig. 4. Relationship between temperature and EMF after irradiation.

thermodynamic data [10]. The EMF of all sensors (MSZ sensor, CSZ sensor, and YSZ sensor) was 5–55% smaller than the reference value, when neutron fluence ( $E > 1$  MeV) increased up to  $8.9 \times 10^{22} \text{ m}^{-2}$ . There is a threshold in decreasing EMF between neutron fluences of  $8.9 \times 10^{21}$  and  $8.9 \times 10^{22} \text{ m}^{-2}$  ( $E > 1$  MeV). It is noteworthy that the decrease in EMF of the CSZ sensor was significantly smaller than those of MSZ and YSZ sensors.

(2) DC resistance measurement: The activation energy of oxygen ion conduction was obtained from the relation between the absolute value of DC resistance and the temperature of the oxygen sensor. These results are shown in Table 1(a).

The activation energy of the oxygen ion was 1.657 eV for the unirradiated YSZ sensor, and was 1.358 eV for the YSZ sensor irradiated to a neutron fluence of

$8.9 \times 10^{22} \text{ m}^{-2}$  ( $E > 1$  MeV). It appears that the mobility of the oxygen ion increased with increase of neutron fluences. The activation energy of the oxygen ion was 0.757 eV for the CSZ sensor irradiated to  $8.9 \times 10^{22} \text{ m}^{-2}$ , and was 1.732 eV for the MSZ sensor irradiated to  $8.9 \times 10^{21} \text{ m}^{-2}$ .

(3) AC impedance measurement: A typical result of AC impedance measurements is shown in Fig. 5, as a Cole–Cole Plot [11]. The semicircle of the neutron-irradiated sensor was lower than that for unirradiated material, and new semicircle was measured. The explanation for this effect seems to be that new relaxation behavior of the electrical dipole is changed by neutron irradiation, or that the hydrogen which  $\text{H}_2\text{O}$  is dissociated into  $\text{H}_2$  and  $\text{O}_2$  by neutron irradiation is adsorbed in the interface of stabilized zirconia and electrode [12].

Table 1  
Activation energies

Samples	Neutron fluence ( $\text{n/m}^{-2}$ )	Activation energy ( $\text{J/mol}$ )	Activation energy (eV)
<i>(a) Activation energy of oxygen ion</i>			
YSZ	Unirrad.	159795	1.657
YSZ	$8.9 \times 10^{22}$	131012	1.358
CSZ	$8.9 \times 10^{22}$	73025	0.757
MSZ	$8.9 \times 10^{21}$	167037	1.732
<i>(b) Activation energy of dipole of stabilized zirconia</i>			
YSZ	Unirrad.	128626	1.334
YSZ	$8.9 \times 10^{22}$	60200	0.624
CSZ	$8.9 \times 10^{22}$	98895	1.025

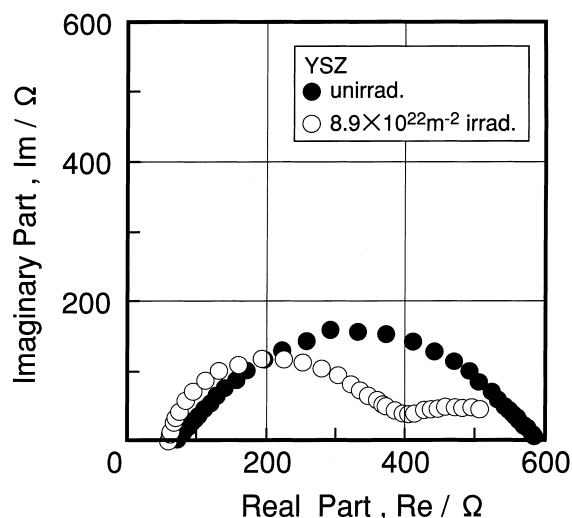


Fig. 5. Cole–Cole Plot at 1123 K after irradiation.

The cause of EMF decrease of the oxygen sensor by neutron radiation can be explained as follows. There is an new electric field was caused in the solid electrolyte of the oxygen sensor by neutron irradiation, and excited free electron by neutron irradiation is brought about. Thus an electron current flows, the oxygen ion conduction decreases [13], and as a result, the EMF of oxygen sensors decreases. Furthermore, the irreversible reaction by decomposition of stabilized zirconia and electrode EMF too.

Activation energies of electrical dipoles were obtained from AC impedance measurements, and are shown in Table 1(b). The activation energy of electrical dipoles was 1.334 eV for the unirradiated YSZ sensor, and was 0.624 eV for the YSZ sensor and 1.025 eV for the CSZ sensor irradiated with neutron fluences of  $8.9 \times 10^{22} \text{ m}^{-2}$  ( $E > 1 \text{ MeV}$ ). It means that the electrical dipole becomes easy to move with increase of neutron fluences. And activation energy of the electrical dipole decreased with increasing neutron fluence and the change in activation energy of CSZ was negligibly smaller than those of YSZ and MSZ. Therefore, the decrease in the EMF of the CSZ sensor was smaller than those of MSZ and YSZ sensors.

#### 4. Conclusion

Characteristics of oxygen sensors were investigated by irradiation tests and post-irradiation tests. Conclusions are summarized as follows.

1. From the irradiation tests, the EMF of YSZ sensor was 231 mV at the start of the test at 973 K. That value was 20% and 60% smaller than the starting value at fluences  $1 \times 10^{22}$  and  $1 \times 10^{23} \text{ m}^{-2}$  ( $E > 1 \text{ MeV}$ ), respectively.
2. From the post-irradiation tests, EMF of the sensors were 5–55% smaller than reference ones when oxygen sensors were irradiated to a neutron fluence of  $9 \times 10^{22} \text{ m}^{-2}$  ( $E > 1 \text{ MeV}$ ). The decrease in the EMF of the CSZ sensor was smaller than that for MSZ and YSZ sensors.
3. Activation energy of the electrical dipole decreased with increasing neutron fluence, and changes in activation energy of CSZ were negligibly smaller than those of YSZ and MSZ.

#### Acknowledgements

We greatly appreciate the helpful comments on this paper by Dr. J. Nakamura (Senior Research Scientist, JAERI) and Dr. O. Baba (Director, Department of JMTR, JAERI). The authors (N.H) would like to thank Professor Z. Kozuka of Fukui Technical College and Mr. H. Kimura of Yamari Industry Corporation, Osaka, Japan, for their helpful discussions and suggestions during this work.

#### References

- [1] C.E. Johnson, K.R. Kummerer, E. Roth, *J. Nucl. Mater.* 188 (1988) 155.
- [2] C.E. Johnson, G.W. Hollenberg, N. Roux, H. Watanabe, *Fusion Eng. Des.* 8 (1989) 145.
- [3] J. Saito, T. Hoshiya, JAERI-Tech 96-015, 1996.
- [4] E. Sugimoto, S. Kuwata, Z. Kozuka, *Japan Institute of Metals* 44 (1980) 644.
- [5] S. Kondo, *Energy Resources* 8 (1987) 509.
- [6] N. Yamazoe, *Electric Chem.* 55 (1987) 200.
- [7] T. Tanaka, *Appl. Phys.* 49 (1980) 956.
- [8] Z. Kozuka, I. Katayama, H. Kosaka, *Japan Institute of Mining* 96-1109 (1980) 477.
- [9] A. Nakamura, T. Fujino, *J. Nucl. Mater.* 149 (1987) 80.
- [10] R.A. Rapp, *Physicochemical Measurements in Metals Research, Part 2*, 1970, pp. 123–192.
- [11] M. Okido, T. Oki, *Japan Inst. Met.* 32 (1993) 199.
- [12] J.F. Baumard, B. Cales, A.M. Anthony, *Ceramic Science and Technology at the Present and in the Future, Japan*, 1981, pp. 161–191.
- [13] K. Fueki, *Chemical Field* 30 (1976) 297.